

Title....

Marcus W. Beck¹, John C. Lehrter¹

¹*USEPA National Health and Environmental Effects Research Laboratory*

Gulf Ecology Division, 1 Sabine Island Drive, Gulf Breeze, FL 32561

Phone: 850-934-2480, Fax: 850-934-2401

Emails: beck.marcus@epa.gov, lehrter.john@epa.gov

Version Date: Wed Jul 6 14:26:40 2016 -0500

Abstract

Bio-geo-chemical models are useful tools in environmental sciences that can guide management and policy-making. Consequently, significant time and resources are spent developing these models in system-specific contexts. The optimization of model parameters to maximize precision, including transferability of these models to different systems, are fundamental concerns in the development and application of these tools. This study describes quantitative limitations of coupled hydrodynamic-ecological modelling by contrasting numeric and ecological certainty with a systematic framework for characterizing parameter sensitivity and identifiability. We evaluate a simple bio-geo-chemical model that is the one-dimensional (1-D) unit of a larger spatio-temporal model of hypoxia on the Louisiana continental shelf of Gulf of Mexico as an example. Results from analysis of the 1-D model are used to infer larger trends in dissolved oxygen dynamics over time, having implications for understanding factors that contribute to environmental conditions that are detrimental to aquatic resources. In particular, we focus on issues of parameter identifiability using local sensitivity analyses to provide quantitative descriptions of numerical constraints on model precision. We argue that quantitative and ecological certainty in model calibration are often at odds and the practitioner must explicitly choose model components to optimize given tradeoffs between the two. We further conclude that numerically optimal parameter sets for models of hypoxia are often small subsets of the complete parameter set because of redundancies in the unique effects of parameter perturbations on model output. As a result, we demonstrate that use of a model for inference into ecological mechanisms of observed or predicted changes in hypoxic condition can be potentially misguided in the absence of quantitative descriptions of identifiability. Although these concerns have been expressed in the literature, they are rarely explicitly addressed or included in model evaluations. In addition to immediate implications for regional models, we provide a framework for describing the effects of parameter uncertainty and identifiability that can be applied to similar models to better inform environmental management.

1 Introduction

1. Simulation/biogeochemical/process-based models overview, contrast with statistical models
2. What models seek to provide - generality, precision, realism [Levins \(1966\)](#), there is a

tradeoff so models are 1) developed in partial independence and dependence on the world and theory, 2) function autonomously from both, or 3) represent both at the same time, from Morrison and Morgan (1999), cited in Ganju et al. (2016). This is similar to the bias-variance tradeoff for statistical models, e.g., overparameterization of a model makes it very biased as it fits the data (the world) exactly, tradeoff between sensitivity and error with changes in model complexity (more complexity is less error but increasing sensitivity) described in Snowling and Kramer (2001)

3. How is model performance/uncertainty evaluated regarding what they should provide - structural, observational, parameter Beck (1987)?
4. Parameter uncertainty as low-hanging fruit - can do post-hoc and from inner to outer level of complexity, parameter uncertainty is the most common, e.g., marine ecological model Mateus and Franz (2015), but stopped short, global sensitivity analysis of eutrophication model Estrada and Diaz (2010)
5. Challenges related to uncertainty - similar to degrees of freedom, identifiability definition from Brun et al. (2001) and need to evaluate identifiability Fasham et al. (2006), Omlin et al. (2001) did a similar analysis with freshwater biogeochem model. Identifiability describes the ability to estimate a parameter in relation to variation among the remaining parameters. A parameter is identifiable if all parameters within the set can be uniquely estimated based on the observed data. Parameters that are unidentifiable typically produce similar model outputs for a given relative perturbation, i.e., the effect of altering one parameter can be undone by altering one or more other parameters. Model calibration will not converge for parameters sets that are unidentifiable.

This study describes a parameter sensitivity analysis to evaluate identifiability for a bio-geo-chemical model of hypoxia for the northern Gulf of Mexico (GOM). We evaluate a simple one-dimensional (1-D) unit of a larger spatial-temporal model to explore relationships between multiple parameter sets and hypoxia dynamics on the Louisiana continental shelf (LCS). The study also provides a general framework for sensitivity analysis and parameter identifiability that can be used on similar mechanistic models. Specifically, an assumption is that models are

generally over-parameterized and only a finite and smaller subset of the larger parameter set can be optimized for a given research question or dataset. We provide explicit guidance for choosing such subsets of the parameter space given constraints on identifiability as directly related to sensitivity analyses. The specific objectives are to 1) identify the parameters that have the greatest influence on dissolved oxygen (O_2) using local sensitivity analysis, 2) quantify the identifiability of subsets of the total parameter space based on sensitivity, 3) provide a set of heuristics for choosing parameters based on sensitivity and parameter categories with the larger mechanistic model, including extension to other state variables, and 4) discuss implications for hypoxia formation in coastal regions, including management strategies for nutrient reduction and use of mechanistic models to inform decision-making. The ‘optimum’ parameter space is defined as the chosen subset that represents the maximum number of identifiable parameters. Here, ‘optimum’ is both a qualitative description based on a research question or management goal and a quantitative objective based on numerical optimization criteria for fitting model output to a calibration dataset. These results can be used to refine existing models or guide application of models to novel contexts, such as downscaling or application to new environments.

2 Methods

2.1 Model description

Low concentrations of dissolved oxygen occur seasonally on the LCS in the northern GOM. These hypoxic events, defined as $<2 \text{ mg L}^{-1}$ ($< 64 \text{ mmol m}^{-3}$ of O_2), occur in bottom waters and are caused by nutrient inputs from the Mississippi-Atchafalaya River Basin (MARB) that drains a significant portion of the continental United States. Nutrient-stimulated primary production in surface waters increases biological oxygen demand in bottom waters as sinking organic matter is decomposed. The hypoxic area averages $15,540 \text{ km}^2$ annually (1993-2015) with minimum concentrations observed from late spring to early fall. Seasonal variation is strongly related to carbon and nutrient export from the MARB (Lohrenz et al. 2008, Bianchi et al. 2010), whereas factors related to hydrologic variation and wind patterns can affect vertical salinity gradients that contribute to the formation of hypoxia (Wiseman et al. 1997).

Three-dimensional numerical simulation models have been developed to describe factors contributing to hypoxia and to predict the effects of management actions or climate scenarios on

future patterns (Fennel et al. 2013, Pauer et al. 2016, Lehrter et al. in review). This study evaluates a recently developed hydrodynamic and ecological model that describes horizontal and vertical transport and mixing of state variables relevant for hypoxia. The Coastal General Ecosystem Model (CGEM) includes elements from the Navy Coastal Ocean Model (Martin 2000) to describe hydrodynamics on the LCS and a biogeochemical model with multiple plankton groups, water-column metabolism, and sediment diagenesis (Eldridge and Roelke 2010). The hydrodynamic component of CGEM provides a spatially-explicit description of hypoxia dynamics using an orthogonal grid with an approximate horizontal resolution of 1.9 km² and twenty equally-spaced vertical sigma layers on the shelf (depth \leq 100 m, with additional hybrid layers at deeper depths). The biogeochemical component includes equations for 36 state variables including six phytoplankton groups (with nitrogen and phosphorus quotas for each), two zooplankton groups, nitrate, ammonium, phosphate, dissolved inorganic carbon, oxygen, silica, and multiple variables for dissolved and particulate organic matter from different sources. The model can be run for a set period of time at a given time step using atmospheric and hydrological boundary conditions described in Hodur (1997) and Lehrter et al. (2013).

The core unit of CGEM is a 1-D model called FishTank that implements the biogeochemical equations in Eldridge and Roelke (2010). This model acts as a standalone operational unit from the 3-D model that does not include any form of transport (i.e., advection, mixing, or surface flux) such that it can easily be applied to other hydrodynamic grids. Accordingly, the sensitivity and identifiability analysis described below are informative for both the LCS gridded model as well as potential applications to different systems. The FishTank model provides estimates for the 36 state variables described above using a 1-D parcel that is uniformly mixed. A set of initial conditions is provided as input to the model that was based on observations of relevant variables obtained from research cruises in April, June, and September 2006 (Table 1, Murrell et al. (2014)). The FishTank model was executed from January 1st to Decemberst, 2006 at a timestep of five minutes.

Results from FishTank are based on time-dependent differential equations that describe energy flow between phytoplankton (up to six groups) and zooplankton (two groups) as affected by nutrient uptake rates, organic matter inputs and losses, inherent optical properties, sediment diagenesis, and temperature (Penta et al. 2008, Eldridge and Roelke 2010, see appendix in Lehrter

et al. in review). A total of 108 equations are estimated at each time step to return a value for each of the 36 state variables described by the model. In addition to the initial conditions, a set of parameter values for each of the equations is also supplied at model execution. These parameters define relationships among fixed effects in the equations and represent ecological properties described by the model that influence hypoxia formation. Values for each of the parameters were based on estimates from the literature, field or laboratory-based measurements, or expert-based knowledge in absence of the former. The sensitivity of O₂ was estimated at each timestep from FishTank in relation to 249 parameters that are included in the 108 equations. For simplicity in the discussion below, the parameters were grouped into one of six categories based on respective equations: optics, organic matter, phytoplankton, temperature, and zooplankton. A full description of the equations and parameters is available as an appendix in (Lehrter et al. in review).

2.2 Local sensitivity analysis

The analysis focused on sensitivity of O₂ in the 1-D FishTank model to identify parameters that may affect spatial and temporal variation of hypoxia in the larger model. A local sensitivity analysis was performed for each of the 249 parameters using a simple perturbation approach to evaluate the change in O₂ from the original parameter values. The analyses relied exclusively on concepts used in the FME package developed for the R statistical programming language (Soetaert and Petzoldt 2010). Each parameter was perturbed by 50% of its original value and the model was executed to obtain an estimate of the effect on O₂. For each perturbation, a sensitivity value S was estimated for each time step i given a set value for parameter j as:

$$S_{ij} = \frac{\partial y_i}{\partial \Theta_j} \cdot \frac{w_{\Theta_j}}{w_{y_i}} \quad (1)$$

where the estimate depended on the change in the predicted value for response variable y divided by the change in the parameter Θ_j multiplied by the quotient of scaling factors w for each. The scaling factors, w_{Θ_j} for the parameter Θ_j and w_{y_i} for response variable y_i , were set as the default value of the unperturbed parameter and the predicted value of y_i after perturbation (Soetaert and Petzoldt 2010). The scaling ensures the estimates are unitless such that the relative magnitudes provide a comparison for model sensitivity to parameter changes that may vary in scale.

Estimates for S_{ij} were summarized as $L1$ and $L2$ across the time series to obtain individual sensitivity values of O_2 in response to a change in parameter j :

$$L1 = \sum |S_{ij}|/n \quad (2)$$

$$L2 = \sqrt{\sum (S_{ij}^2)/n} \quad (3)$$

In general, positive sensitivity estimates suggested a parameter had a positive effect on O_2 for a given increase in the parameter, whereas the converse was true for negative sensitivity estimates. However, the effect of a parameter change may not be uniform over time such that S_{ij} can change in magnitude and sign depending on the location. Time series of O_2 estimates before and after perturbation were also evaluated to identify patterns not captured by the summary statistics. All parameters for each of the six equation categories (optics, organic matter, phytoplankton, temperature, and zooplankton) that had non-zero $L1$ or $L2$ were retained for identifiability analysis.

2.3 Identifiability and selecting parameter subsets

Identifiability of parameter subsets was estimated from the minimum eigenvector of the cross-product of a selected sensitivity matrix (Brun et al. 2001, Omlin et al. 2001):

$$\gamma = \frac{1}{\sqrt{\min(\text{EV}[\hat{S}^\top \hat{S}])}} \quad (4)$$

where γ ranges from one to infinity for perfectly identifiable (orthogonal) or unidentifiable (perfectly collinear) results for a set of parameters in a chosen sensitivity matrix S . The sensitivity functions were supplied as a matrix \hat{S} with rows i and columns j (eq. (1)) that describes deviations of predicted O_2 from the default parameter values. The matrix \hat{S} was first normalized by dividing by the square root of the summed residuals (Omlin et al. 2001, Soetaert and Petzoldt 2010).

The collinearity index γ provides a measure of the linear dependence between sensitivity functions described above for subsets of parameters. Estimates of γ greater than 10-15 suggest parameter sets are poorly identifiable (Brun et al. 2001, Omlin et al. 2001), meaning optimal values are inestimable given similar effects of the selected parameters on O_2 . Greater sensitivity

of a state variable to parameters within a subset does not imply identifiability if the individual effects are similar. An intuitive interpretation of γ is provided by Brun et al. (2001) such that a change in a state variable caused by a change in one parameter can be offset by the fraction $1 - 1/\gamma$ by the remaining parameters. That is, $\gamma = 10$ suggests the relative change in O_2 for a selected parameter can be compensated for by 90% with changes in the other parameters.

Initial analyses suggested that considerably limited subsets of parameters were identifiable of the 249 included in the FishTank model. Given this limitation, parameter selection must consider the competing objectives of increased precision with parameter inclusion and identifiability as it relates to optimization. An additional challenge is the excessively high number of combinations of parameter sets, which complicates selection given differences in parameter sensitivity and desired ecological categories of each parameter as they relate to the biogeochemical equations. For example, Fig. 1 provides a simple graphic of the unique number of combinations that are possible for different subsets of ‘complete’ parameter sets of different sizes (i.e., based on n choose k combinations equal to $n! / (k! (n - k)!)$). The number of unique combinations increases with the total parameters in the set and is also maximized for moderate selections (e.g., selecting half the total). For example, over 10^{14} combinations are possible by selecting 25 parameters from a set of 50. Accordingly, parameter selection is complicated by differing sensitivity, identifiability, and the difficulty of choosing from many combinations.

A set of heuristics was developed to balance the tradeoff in model complexity and identifiability given the challenges described above. These rulesets were developed with the assumption that parameters will be selected given preference for those with high sensitivity and identifiability based on $\gamma < 15$ was an acceptable threshold for subsets (e.g., 93% accountability between parameters). Selection heuristics also recognized that parameter categories (i.e., optics, organic matter, phytoplankton, temperature, zooplankton) may have unequal preferences given questions of interest. In all selection scenarios, parameters were selected by decreasing sensitivity starting with the most sensitive until identifiability did not exceed $\gamma = 15$ where selections were 1) blocked within parameter category, 2) independent of parameter category, 3) or considering all categories equally. The selection rules produced seven subsets of parameters that could further be used to optimize model calibration for O_2 .

Finally, the above analyses were repeated for additional state variables estimated by

FishTank to provide further descriptions of ecological dynamics that are relevant for hypoxia. In addition to O_2 , other state variables included chlorophyll *a* (*chl-a*), photosynthetically active radiation (PAR), nitrate, ammonium, particulate organic matter, dissolved organic matter, and phosphorus. Particulate and dissolved organic matter were estimated as the summation of the respective outputs for organic matter from phytoplankton (*OM1_A*, *OM2_A*), fecal pellets (*OM1_fp*, *OM2_fp*), river sources *OM1_rp*, *OM2_rp*), and boundary conditions (*OM1_bc*, *OM2_bc*, see [Lehrter et al. in review](#)).

3 Results

3.1 Local sensitivity analysis

Tables 1 to 5, how many parameters in each category, how many induced a response in O_2 , what parameters in each category had the greatest sensitivity (Fig. 2), what were sensitivity magnitudes between categories, did these vary by phyto or zoop groups?

Plotting the raw values from the sensitivity analysis provides a visual assessment of changes (Fig. 2).

Fig. 3 shows identifiability ranges, describe by category, also emphasize that selection independent of category may be more appropriate (better identifiability). Jumps in median suggest inclusion of a specific parameter has disproportionate affect on identifiability.

Note that identifiability for one phytoplankton group and one zooplankton group needs to be evaluated, lots of redundancy between groups.

Reading each plot from left to right can be interpreted as including additional parameters, where each parameter is ranked by relative sensitivity. The inset in each plot shows the identifiability of including parameters, up to a maximum where additional inclusion exceeds the identifiability threshold of fifteen. The scenarios for including parameters all begin with the parameters that have the greatest effect on the model output. The inclusion of additional parameters depends on the scenario. The first scenario selected parameters by decreasing sensitivity within each category (i.e., four separate models calibrated for optics, organics, phytoplankton, or zooplankton), the second scenario selected parameters by sensitivity regardless of category, and the third scenario selects parameters by sensitivity with equal representation between categories.

4 Discussion

Questions specific to GOM - what initial conditions are important? How many phytoplankton groups do we need (e.g., related to structural uncertainty)?

How does the assimilation of additional parameters (e.g., other state variables) during calibration influence the conclusions?

How does uncertainty translate to what a model should provide (generality v precision)?
The first step - find out what can be optimized but then do not overfit....

What about structural uncertainty - does sensitivity of a model to variation in a parameter imply parameter uncertainty and/or structural uncertainty?

A final point about optimization with identifiable parameter sets - optimization to fit the data still does not ensure a correct model. Failing in one way can be over-compensated by another feature, e.g., the parameter set that is optimized (see [Flynn \(2005\)](#), p. 1207, third paragraph)

[Omlin et al. \(2001\)](#) state that the sensitivity, identifiability, estimation process is iterative (p. 113), need to rinse and repeat for proper calibration.

How to improve identifiability - get more/better observed data, include obs from other state variables in RSS minimization (eqn q in [Omlin et al. \(2001\)](#))

Alternative methods for uncertainty analysis - bayesian, MCMC, nonlinear calibration-constrained optimization ([Gallagher and Doherty 2007](#))

References

- Beck MB. 1987. Water quality modeling: A review of the analysis of uncertainty. *Water Resources Research*, 23(8):1393–1442.
- Bianchi TS, DiMarco SF, Jr JHC, Hetland RD, Chapman P, Day JW, Allison MA. 2010. The science of hypoxia in the Northern Gulf of Mexico: a review. *Science of the Total Environment*, 408(7):1471–1484.
- Brun R, Reichert P, Künsch HR. 2001. Practical identifiability analysis of large environmental simulation models. *Water Resources Research*, 37(4):1015–1030.
- Eldridge PM, Roelke DL. 2010. Origins and scales of hypoxia on the Louisiana shelf: importance of seasonal plankton dynamics and river nutrients and discharge. *Ecological Modelling*, 221(7):1028–1042.
- Estrada V, Diaz M. 2010. Global sensitivity analysis in the development of first principle-based eutrophication models. *Environmental Modelling and Software*, 25:1539–1551.
- Fasham MJR, Flynn KJ, Pondaven P, Anderson TR, Boyd PW. 2006. Development of a robust marine ecosystem model to predict the role of iron in biogeochemical cycles: A comparison of results for iron-replete and iron-limited areas, and the SOIREE iron-enrichment experiment. *Deep-Sea Research I*, 53:333–366.
- Fennel K, Hu J, Laurent A, Marta-Almeida M, Hetland R. 2013. Sensitivity of hypoxia predictions for the norther Gulf of Mexico to sediment oxygen consumption and model nesting. *Journal of Geophysical Research: Oceans*, 118(2):990–1002.
- Flynn KJ. 2005. Castles built on sand: dysfunctionality in plankton models and the inadequacy of dialogue between biologists and modellers. *Journal of Plankton Research*, 27(12):1205–1210.
- Gallagher M, Doherty J. 2007. Parameter estimation and uncertainty analysis for a watershed model. *Environmental Modelling and Software*, 22(7):1000–1020.
- Ganju NK, Brush MJ, Rashleigh B, Aretxabaleta AL, del Barrio P, Grear JS, Harris LA, Lake SJ, McCardell G, O'Donnell J, Ralston DK, Signell RP, Testa JM, Vaudrey JMP. 2016. Progress and challenges in coupled hydrodynamic-ecological estuarine modeling. *Estuaries and Coasts*, 39(2):311–332.
- Hodur RM. 1997. The Naval Research Laboratory's Coupled Ocean/Atmosphere Mesoscale Prediction System (COAMPS). *Monthly Weather Review*, 125:1414–1430.
- Lehrter JC, Ko DS, Lowe L, Penta B. In review. Predicted effects of climate change on the severity of northern Gulf of Mexico hypoxia. In: Justic et al., editor, *Modeling Coastal Hypoxia: Numerical Simulations of Patterns, Controls, and Effect of Dissolved Oxygen Dynamics*. Springer, New York.

- Lehrter JC, Ko DS, Murrell MC, III JDH, Schaeffer BA, Greene RM, Gould RW, Penta B. 2013. Nutrient distributions, transports, and budgets on the inner margin of a river-dominated continental shelf. *Journal of Geophysical Research*, 118(10):4822–4838.
- Levins R. 1966. The strategy of model building in population biology. *American Scientist*, 54(4):421–431.
- Lohrenz SE, Redalje DG, Cai WJ, Acker J, Dagg M. 2008. A retrospective analysis of nutrients and phytoplankton productivity in the Mississippi River plume. *Continental Shelf Research*, 28(12):1466–1475.
- Martin PJ. 2000. Description of the navy coastal ocean model version 1.0. Technical Report NRL/FR/7322-00-9962, Naval Research Lab, Stennis Space Center, Mississippi.
- Mateus MD, Franz G. 2015. Sensitivity analysis in a complex marine ecological model. *Water*, 7:2060–2081.
- Morrison M, Morgan MS. 1999. Models as mediating agents. In: Morgan MS, Morrison M, editors, *Models as Mediators*, page 401. Cambridge University Press, Cambridge.
- Murrell MC, Beddick DL, Devereux R, Greene RM, III JDH, Jarvis BM, Kurtz JC, Lehrter JC, Yates DF. 2014. Gulf of Mexico hypoxia research program data report: 2002-2007. Technical Report EPA/600/R-13/257, US Environmental Protection Agency, Washington, DC.
- Omlin M, Brun R, Reichert P. 2001. Biogeochemical model of Lake Zürich: sensitivity, identifiability and uncertainty analysis. *Ecological Modelling*, 141(1-3):105–123.
- Pauer JJ, Feist TJ, Anstead AM, DePetro PA, Melendez W, Lehrter JC, Murrell MC, Zhang X, Ko DS. 2016. A modeling study examining the impact of nutrient boundaries on primary production on the Louisiana continental shelf. *Ecological Modelling*, 328:136–147.
- Penta B, Lee Z, Kudela RM, Palacios SL, Gray DJ, Jolliff JK, Shulman IG. 2008. An underwater light attenuation scheme for marine ecosystem models. *Optical Express*, 16(21):16581–16591.
- Snowling SD, Kramer JR. 2001. Evaluating modelling uncertainty for model selection. *Ecological Modelling*, 138:17–30.
- Soetaert K, Petzoldt T. 2010. Inverse modelling, sensitivity, and Monte Carlo analysis in R using package FME. *Journal of Statistical Software*, 33(3):1–28.
- Wiseman WJ, Rabalais NN, Turner RE, Dinnel SP, MacNaughton A. 1997. Seasonal and interannual variability within the Louisiana coastal current: stratification and hypoxia. *Journal of Marine Systems*, 12(1-4):237–248.

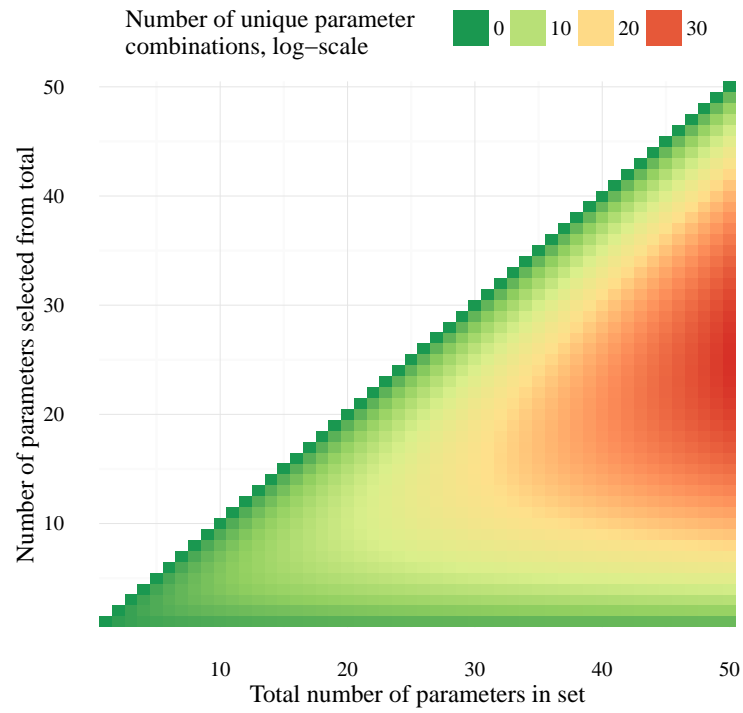


Fig. 1: Examples of unique parameter combinations from different parameter sets and number of selected parameters. The number of combinations are shown for increasing numbers of selected parameters from the total in the set, where 50 parameter sets are shown each with one through 50 total parameters. Note that the number of unique combinations is shown as the natural-log.

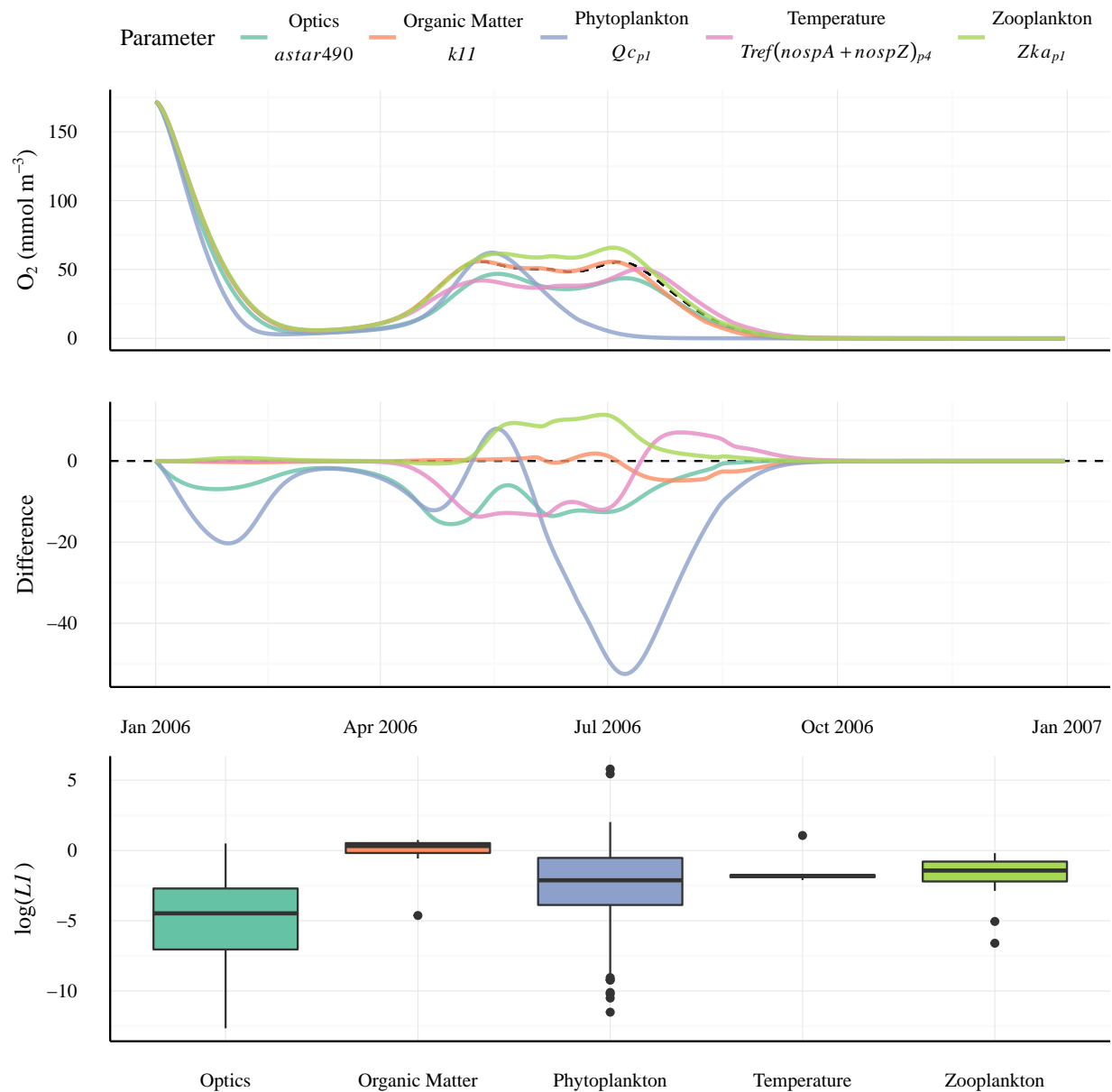


Fig. 2: Sensitivity of O_2 to parameter changes. The solid lines show the change in O_2 based on a 50% change from the default parameter values (dashed line) for each parameter. Individual parameters with the largest effect are shown for each category. The top plot shows the model output and the middle plot shows the estimated O_2 as a difference from the default. The bottom plot shows the distribution of error values (as $\log(L1)$) for all parameters in each category.

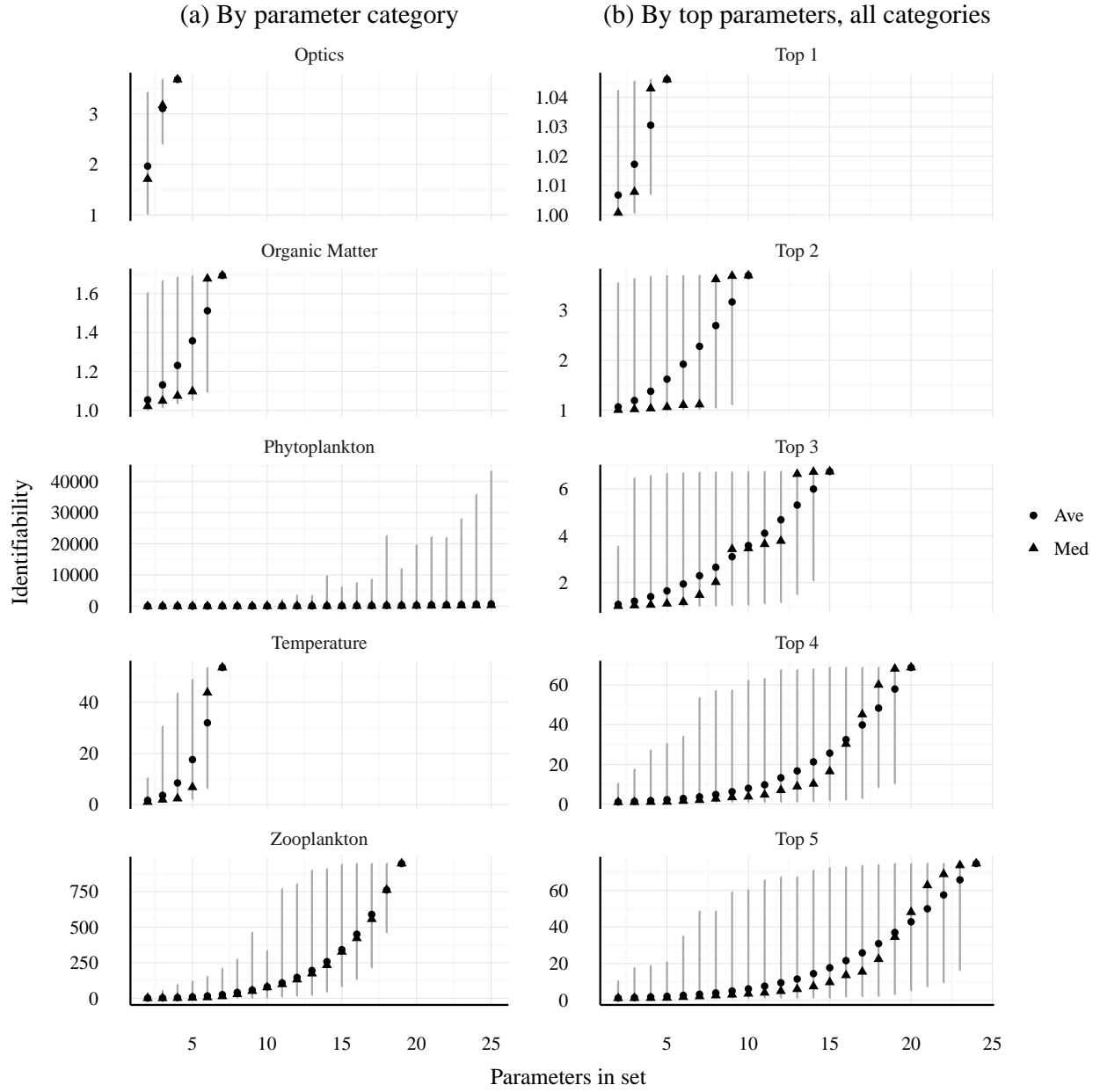


Fig. 3: Identifiability (as γ , eq. (4)) of parameter subsets for O_2 . Plots in (a) show identifiability by parameter categories and (b) shows identifiability by selecting the top 1 through 5 parameters regardless of category. Lines represent identifiability ranges for the possible combinations given the number of parameters in the set. The phytoplankton category is limited to 25 total parameters.

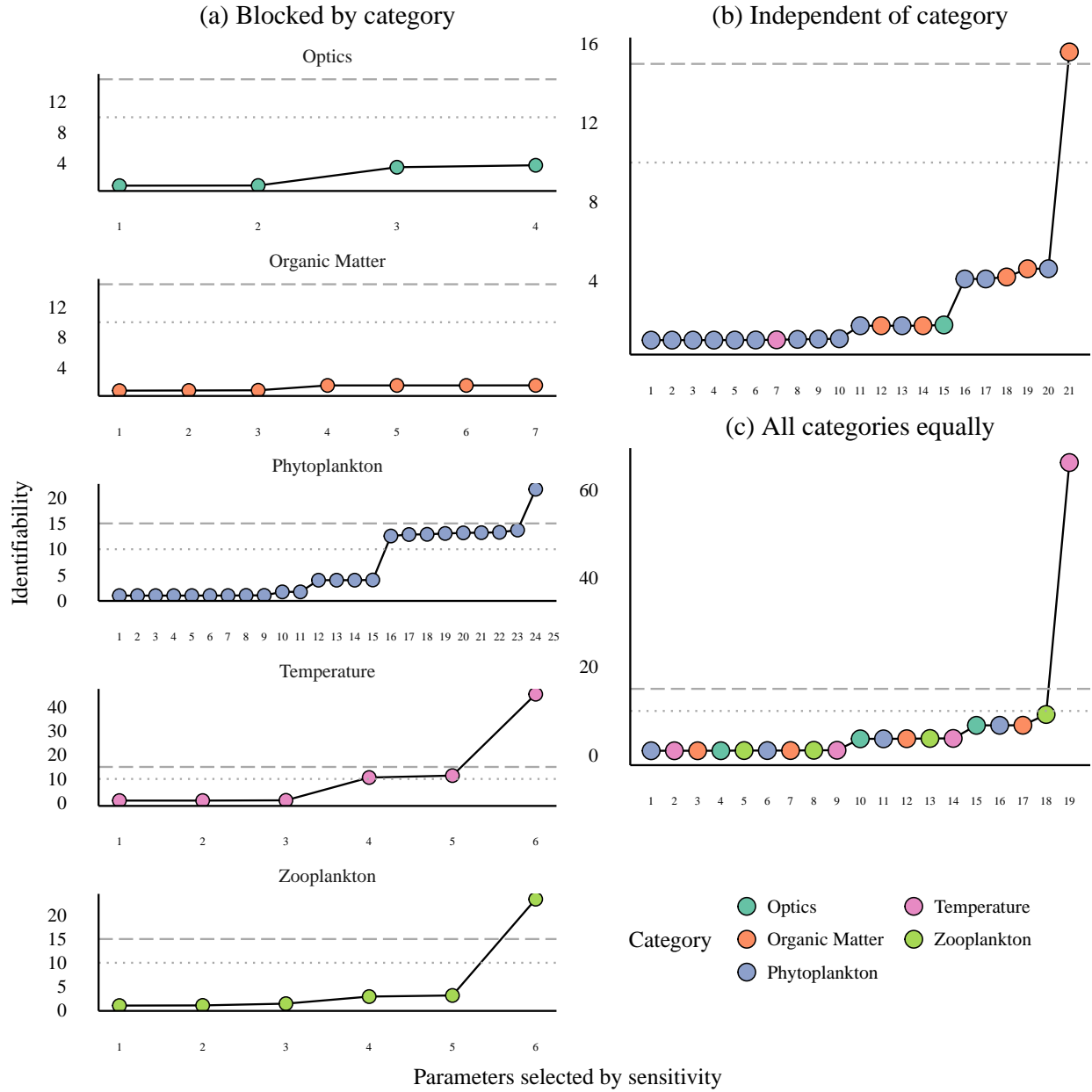


Fig. 4: Identifiability (as γ , eq. (4)) of selecting parameters with three different heuristics. Parameters are selected by decreasing sensitivity for all examples (Tables 1 to 5). The parameter selections are blocked within each category (a), independent of category (b), or considering all categories equally (c). Grey lines indicate potential thresholds at $\gamma = 10, 15$ for maximum acceptable identifiability. Selection stops after $\gamma > 15$ or if the maximum number of possible parameters is selected.

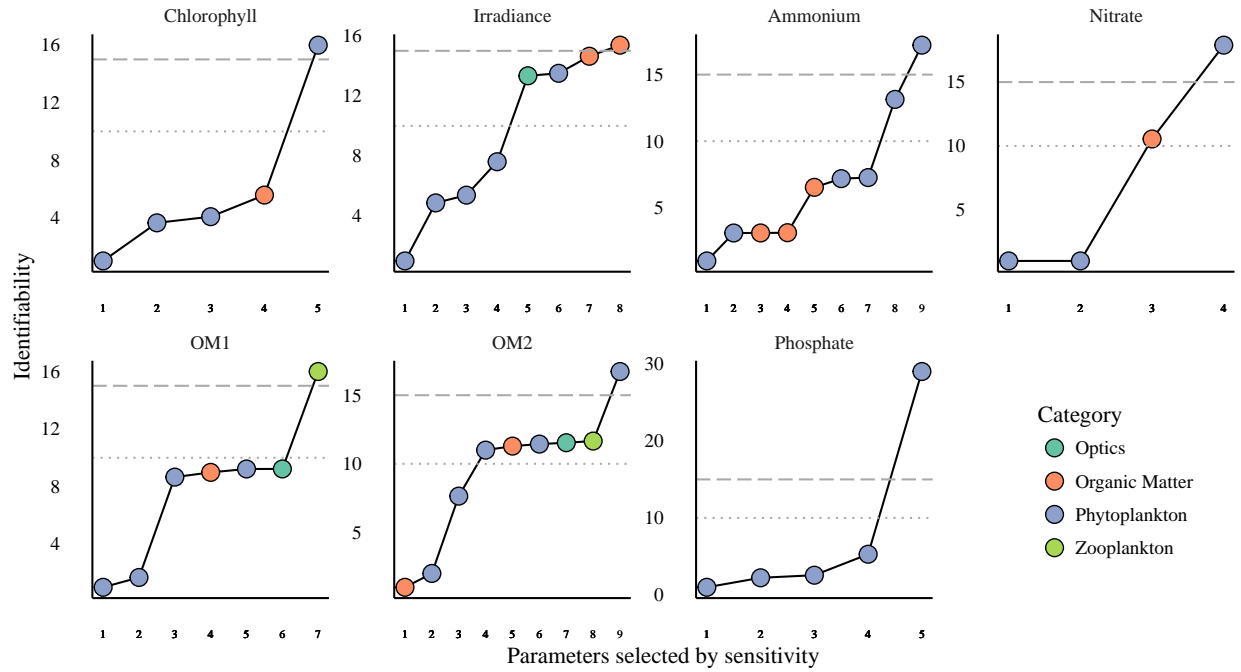


Fig. 5: Identifiability (as γ , eq. (4)) of selecting parameters for selected state variables. Parameters are selected by decreasing sensitivity independent of parameter categories. Grey lines indicate potential thresholds at $\gamma = 10, 15$ for maximum acceptable identifiability. Selection stops after $\gamma > 15$.

Table 1: Sensitivities of O_2 to perturbation of optics parameters. Sensitivities are based on a 50% increase from the default parameter value, where $L1$ and $L2$ summarize differences in model output from the default (see eqs. (2) and (3)). Parameters that did not affect O_2 are not shown.

Description	Parameter	Value	L1	L2
Chla specific absorption at 490 nm	<i>astar490</i>	0.04	1.64	8.64
OMA specific absorption at 490 nm	<i>astarOMA</i>	0.1	0.02	0.1
OMZ specific absorption at 490 nm	<i>astarOMZ</i>	0.1	0.01	0.01
AOP, light attenuation due to CDOM	<i>Kcdom</i>	0	3.18×10^{-6}	1.09×10^{-5}

Table 2: Sensitivities of O_2 to perturbation of organic matter parameters. Sensitivities are based on a 50% increase from the default parameter value, where $L1$ and $L2$ summarize differences in model output from the default (see eqs. (2) and (3)). Parameters that did not affect O_2 are not shown.

Description	Parameter	Value	L1	L2
rate constant for nitrification	<i>kII</i>	5	2.11	16.1
O_2 concentration that inhibits denitrification	<i>KstarO2</i>	10	1.91	11.76
turnover rate for OM1A and OM1G	<i>KG1</i>	50	1.49	6.83
turnover rate for OM2A and OM2G	<i>KG2</i>	50	1.37	3.46
half-saturation concentration for NO_3 used in denitrification	<i>KNO3</i>	10	1.24	7.98
half-saturation concentration for O_2 utilization	<i>KO2</i>	10	0.56	1.92
decay rate of CDOM, 1/day	<i>KGcdom</i>	0.01	0.01	0.03

Table 3: Sensitivities of O_2 to perturbation of phytoplankton parameters. Sensitivities are based on a 50% increase from the default parameter value, where $L1$ and $L2$ summarize differences in model output from the default (see eqs. (2) and (3)). Parameters that did not affect O_2 are not shown. Subscripts show the phytoplankton or zooplankton group that applies for the parameter. Parameters less than the 75th percentile (0.59) for $L1$ were removed for brevity.

Description, Parameter	Value	L1	L2
coefficient for non-limiting nutrient			
aN_{P1}	1	2.7	47.26
aN_{P3}	1	0.66	3.16
half-saturation constant for N			
Kn_{P3}	5.93	1.15	9.22
Kn_{P4}	1.13	0.62	2.5
initial slope of the photosynthesis-irradiance relationship			
α_{P4}	3.96×10^{-16}	1.61	7.46
α_{P3}	6.19×10^{-17}	1.06	3.74
α_{P5}	3.87×10^{-16}	0.81	5.54
minimum N cell-quota			
$QminN_{P3}$	1.27×10^{-8}	1.53	6.4
$QminN_{P4}$	1.53×10^{-10}	0.91	2.76
$QminN_{P1}$	6.08×10^{-9}	0.62	4.55
mortality coefficient			
mA_{P3}	0.03	2.98	14.34
mA_{P4}	0.11	1.35	7.04
N-uptake rate measured at u_{max}			
$vmaxN_{P5}$	1.4×10^{-9}	7.57	43.9
$vmaxN_{P4}$	1.33×10^{-9}	2.88	16.56
$vmaxN_{P3}$	8.11×10^{-8}	1.99	15.23
$vmaxN_{P1}$	4.1×10^{-8}	0.84	2.92
P-uptake rate measured at u_{max}			
$vmaxP_{P3}$	6.15×10^{-8}	2.23	9.89
$vmaxP_{P1}$	2.68×10^{-8}	0.74	11.41
phytoplankton basal respiration coefficient			
$respb_{P4}$	0.02	3.1	26.48
$respb_{P3}$	0.02	2.15	6.35
$respb_{P5}$	0.02	0.81	8.61
phytoplankton carbon/cell			
QC_{P1}	1.35×10^{-6}	328.35	2181.05
QC_{P3}	2.65×10^{-6}	232.8	1574.72
QC_{P2}	1.68×10^{-7}	4.08	61.25
QC_{P4}	4.54×10^{-8}	1.03	3.75
phytoplankton growth respiration coefficient			
$resp_{P4}$	0.1	0.98	7.37

Table 4: Sensitivities of O_2 to perturbation of temperature parameters. Sensitivities are based on a 50% increase from the default parameter value, where $L1$ and $L2$ summarize differences in model output from the default (see eqs. (2) and (3)). Parameters that did not affect O_2 are not shown. Subscripts show the phytoplankton or zooplankton group that applies for the parameter.

Description, Parameter	Value	L1	L2
Optimum temperature for growth(C)			
$T_{ref}(nospA+nospZ)_{P4}$	17	2.9	22.95
$T_{ref}(nospA+nospZ)_{Z2}$	26	0.18	2.59
$T_{ref}(nospA+nospZ)_{P5}$	26	0.17	0.72
$T_{ref}(nospA+nospZ)_{P2}$	22	0.16	0.82
$T_{ref}(nospA+nospZ)_{Z1}$	22	0.16	0.33
$T_{ref}(nospA+nospZ)_{P3}$	17	0.14	0.78
$T_{ref}(nospA+nospZ)_{P1}$	22	0.12	0.29

Table 5: Sensitivities of O_2 to perturbation of zooplankton parameters. Sensitivities are based on a 50% increase from the default parameter value, where $L1$ and $L2$ summarize differences in model output from the default (see eqs. (2) and (3)). Parameters that did not affect O_2 are not shown. Subscripts show the phytoplankton or zooplankton group that applies for the parameter.

Description, Parameter	Value	L1	L2
assimilation efficiency as a fraction of ingestion			
$Z_{effic_{P1}}$	0.4	0.23	0.55
$Z_{effic_{P2}}$	0.4	0.21	0.75
half saturation coefficient for grazing			
$ZK_{a_{P1}}$	1.12×10^{12}	0.82	6.29
$ZK_{a_{P2}}$	1.12×10^{12}	0.46	3.24
maximum growth rate of zooplankton			
$Z_{max_{P2}}$	2.98×10^7	0.48	1.84
$Z_{max_{P1}}$	9.45×10^8	0.46	0.91
proportion of grazed phytoplankton lost to sloppy feeding			
$Z_{slop_{P1}}$	0.25	0.12	0.33
Zooplankton biomass-dependent respiration factor			
$Z_{resp_{P1}}$	0.1	0.45	3.02
$Z_{resp_{P2}}$	0.42	0.09	1.05
zooplankton carbon/individual			
$ZQ_{C_{P2}}$	7.08×10^{-7}	0.1	0.36
$ZQ_{C_{P1}}$	3.13×10^{-4}	0.06	0.62
Zooplankton growth-dependent respiration factor			
$Z_{resp_{g_{P1}}}$	0.2	0.24	3.19
$Z_{resp_{g_{P2}}}$	0.3	0.12	0.31
Zooplankton mortality constant for quadratic mortality			
Zm_{P2}	7.2×10^{-4}	0.33	2.85
Zm_{P1}	7.2×10^{-4}	0.26	0.8
zooplankton nitrogen/individual			
$ZQ_{n_{P1}}$	6.95×10^{-5}	0.47	1.64
$ZQ_{n_{P2}}$	1.57×10^{-7}	0.24	1.35
zooplankton phosphorus/individual			
$ZQ_{p_{P2}}$	8.53×10^{-9}	0.01	0.01
$ZQ_{p_{P1}}$	3.77×10^{-6}	0	0